Macromolecules

Article

pubs.acs.org/Macromolecules

Glycopolymer-Grafted Nanoparticles: Synthesis Using RAFT Polymerization and Binding Study with Lectin

S. N. Raju Kutcherlapati, Rambabu Koyilapu, Uma Maheswara Rao Boddu, Debparna Datta, Ramu Sridhar Perali,* Musti J. Swamy,* and Tushar Jana*

School of Chemistry, University of Hyderabad, Hyderabad, India

Supporting Information

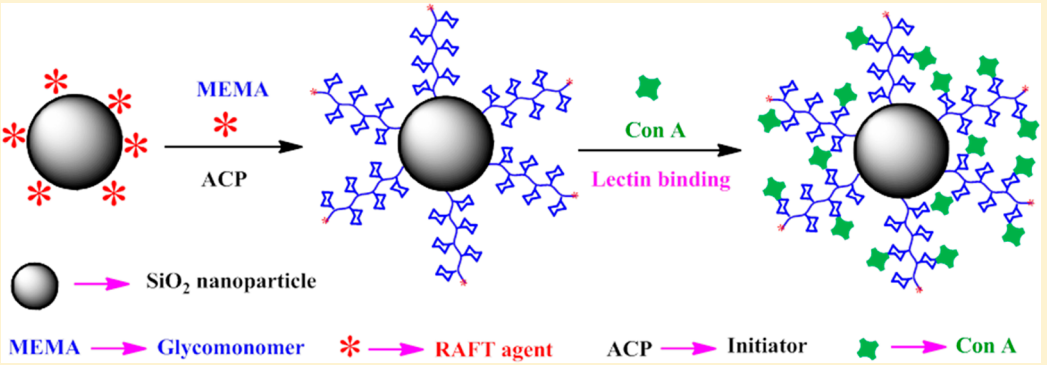

ABSTRACT: The weak binding between carbohydrates and proteins is a major constraint toward the development of carbohydrate-based therapeutics. To address this, here we report the synthesis of glycopolymer (GP)-grafted silica nanoparticles (SiNP) by using reversible addition−fragmentation chain transfer (RAFT) polymerization through the *grafting-from* approach using a multistep process. GP chains of various lengths with controlled molecular weight and narrow polydispersities were grown on the RAFT agent anchored SiNP surface using mannosyloxyethyl methacrylate (MEMA) as a glycomonomer. Spectroscopic (FT-IR, NMR) and thermogravimetric studies confirmed the grafting of poly(MEMA) chains on the SiNP surface and also showed that the dry DMF is a better solvent as compared to water/ethanol mixture for carrying out the MEMA polymerization on SiNP surface. The mean diameter of the dry GP-grafted SiNPs (GP-*g*-SiNPs) obtained from microscopic studies was in the range 50−60 nm, whereas the hydrodynamic diameter as obtained using light scattering measurements varied between 90 and 165 nm depending on the chain length of poly(MEMA). Hydrolysis of silica cores using aqueous HF enabled characterization of cleaved polymer using GPC, and the obtained unimodal chromatogram and narrow PDI confirmed that the polymerization proceeded through the RAFT mechanism. GP-*g*-SiNPs displayed stronger binding to the mannose specific lectin, Concanavalin A, owing to the larger positive binding entropic contribution which resulted in an association constant that is 800- and 400-fold stronger than that of monomeric mannose and GP chains, respectively.

INTRODUCTION

Often, the association between carbohydrates and proteins is recognized as low-affinity binding, which can be enhanced by creating multivalent interactions using multiple carbohydrate ligands. This approach can lead to increase in the interactions (in terms of binding constant of protein−carbohydrates) by manifold than that of corresponding monovalent interaction.[1−5] A polymeric chain in which carbohydrate groups are hanging from the main backbone can act as multiple carbohydrate ligands and be termed as glycopolymer (GP).

The synthesis of glycopolymers (GPs) with different architecture is an important step toward the understanding of interactions between GPs and proteins and more importantly for unraveling the influence of GPs architecture on the binding with proteins.[6−8] Hence, there is a need to develop a versatile method for the preparation of GPs especially in such a structural form (architecture) which eases the conjugation with proteins. One can hypothesize that GP chains grafted on the surface of nanoparticles might be the right choice for easy and strong conjugation with protein/lectin since a large number of GP chains on the nanoparticle surface would be available for binding with protein which will perhaps enhance the binding capability. However, this objective can only be realized if one can grow the GP chains on the nanoparticle surface.

Among several nanoparticle surfaces which can be used to graft GP chain, silica nanoparticles (SiNP) in particular provide several interesting advantages like biocompatibly, low toxicity, and readily functionalizable surface when compared with heavy metals and other types of metallic/semiconducting surfaces.[9−12] In the literature, carbohydrate modified nanoparticles (includ-

Received: June 14, 2017
Revised: August 2, 2017

DOI: 10.1021/acs.macromol.7b01265
Macromolecules XXXX, XXX, XXX−XXX

Scheme 1. Synthesis of Mannose-Capped Hydroxyethyl Methacrylate (MEMA)[a]

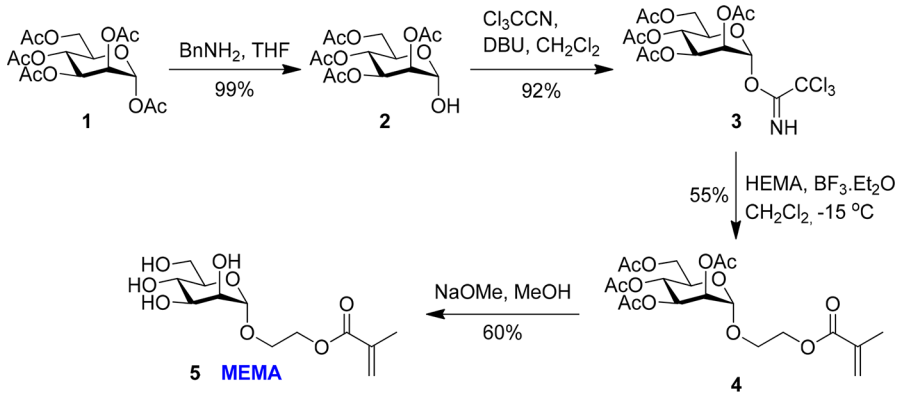

[a]This molecule is used as a monomer to grow the GP chain.

Scheme 2. Synthesis of 4-Cyanopentanoic Acid Dithiobenzoate (CPDB)-Modified Silica Nanoparticles (SiNP-CPDB)

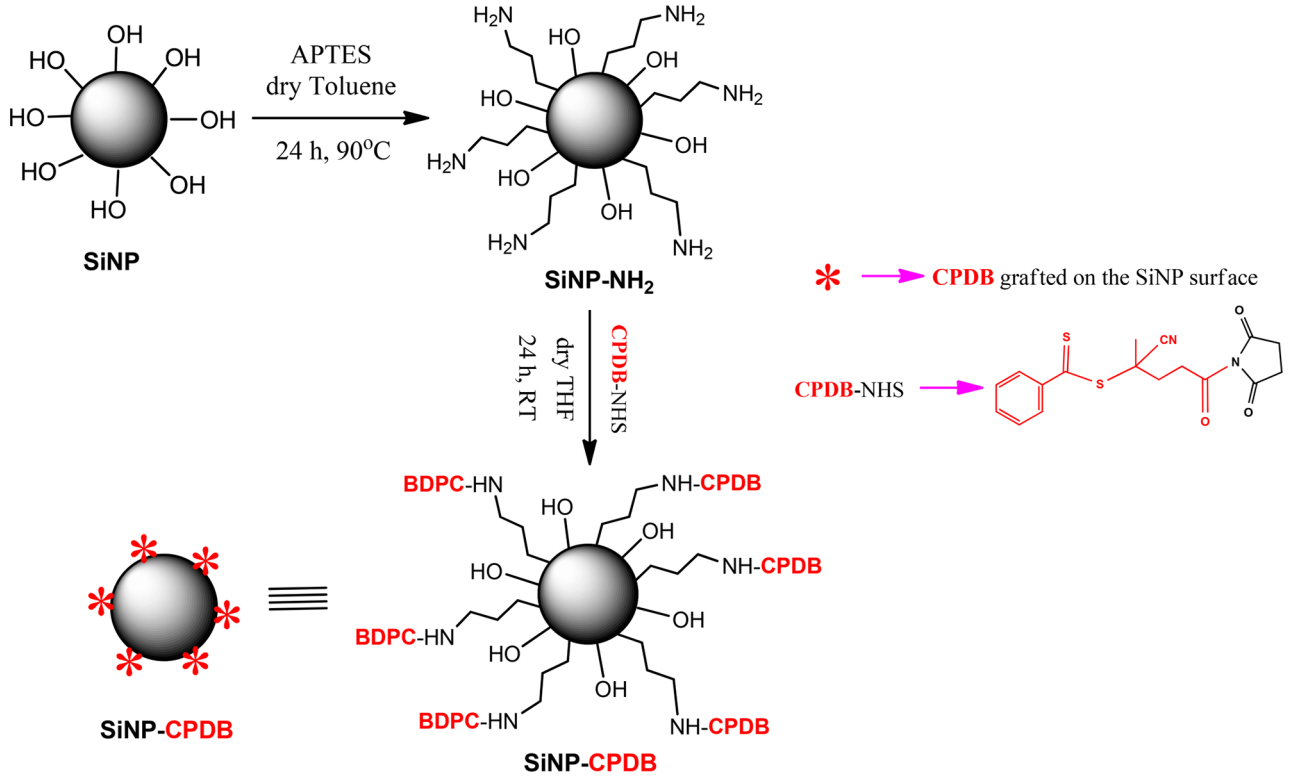

ing SiNPs) have recently attracted much attention for understanding lectin−carbohydrate interactions and find applications in a variety of biological processes including fertilization, cell migration, cancer therapy, and host−pathogen interactions.[7,8,13−24]

Grafting of carbohydrates on the surface of SiNPs has been carried out using a variety of conjugation techniques, including copper-catalyzed azide−alkyne cycloaddition (CuAAC), amide coupling, nucleophilic substitution, and photocoupling.[13,25] The majority of these methods typically involve laborious multistep procedures as well as costly and potentially toxic metal catalysts. Also, these methodologies cannot be used to graft GP chains since they are synthesized with protected glycomonomers to avoid unnecessary hydrolysis during polymerization, and deprotection is carried out after polymerization. Few unprotected glycomonomers have been polymerized on the silica surface through surface-initiated polymerization.[26−28] The whole process of protection−deprotection on the SiNP surface can become very tedious, and hence, there is a need to develop an alternative and novel method for grafting of GP chains on the SiNP surface. Two methods namely *grafting-to* and *grafting-from* are mostly used for modification of nanoparticle surfaces with polymers.[29−34] In the case of the *grafting-to* method, polymer chains are grafted to the nanoparticle surface whereas the grafting reaction is conducted by polymerizing monomers from the nanoparticle surface in the case of the *grafting-from* method. Both these methods have certain advantages along with few limitations and have been used in the literature to produce a thin polymer layer on the nanoparticle surface. Although the *grafting-to* method is simple to be performed, the obtained graft density is fairly low since the diffusion of polymer chains to the particle surface is

DOI: 10.1021/acs.macromol.7b01265
Macromolecules XXXX, XXX, XXX−XXX

sterically hindered. Therefore, we believe the *grafting-from* method to grow the GP chain onto the SiNP surface would be the better choice for obtaining high graft density of GP chains.

Among the controlled radical polymerizations (CRPs), reversible addition−fragmentation chain transfer polymerization (RAFT) is highly popular for grafting polymers on particle surfaces owing to the advantages of being compatible with a wide range of monomers including functional monomers, free of transition metal ion contamination and mild reaction conditions.[35−41]

With this background as discussed above and to the best of our knowledge no report has appeared until now on the grafting of GP chains on the SiNP surface using the *grafting-from* RAFT polymerization method which will allow control over molecular weights, chain length, and grafting density and hence the morphology of resulting materials, which in turn can have a significant influence on protein binding. Therefore, in this work, we report the synthesis of structurally well-defined, glycopolymer-grafted SiNP (GP-*g*-SiNP) hybrid materials by modifying the surface of SiNP with suitable RAFT agent and then chain extended with glycomonomer to produce GP-grafted SiNPs. The monomer used in this study is the mannose derivative (mannosyloxyethyl methacrylate, MEMA) which has strong lectin binding activity. In addition to synthesis, characterization, and structural elucidation of GP-*g*-SiNP, we have studied the lectin binding of this nanomaterial with Concanavalin A (Con A) using isothermal titration calorimetry (ITC).

EXPERIMENTAL SECTION

Synthesis of 2-(α-D-Mannosyloxy)ethyl Methacrylate (MEMA, 5) Monomer. MEMA was synthesized by following the reaction scheme shown in Scheme 1. Detailed synthetic protocols and characterization data of compounds **2**, **3**, and **4** are described in the Supporting Information. Conversion of compound **4** to the final monomer MEMA (compound **5**) was carried out as described below. A solution of 2-*O*-(2′,3′,4′,6′-tetra-*O*-acetyl-α-D-mannosyl)ethyl methacrylate **4** (11 g, 23.89 mmol) and freshly prepared sodium methoxide (22 mL, 0.01 M) in anhydrous methanol (110 mL, 0.1 g/mL) were stirred under a nitrogen atmosphere for 15 min at room temperature. After this, the reaction mixture was neutralized to pH ∼ 7 with DOWEX8W50 ion-exchange resin. The solution was filtered, and the solvent was removed under vacuum. The obtained crude compound was subjected to silica gel column chromatography (20% MeOH in chloroform) to give MEMA **5** (5.76 g, 80%) as colorless solid. R_f 0.5 (MeOH:chloroform, 2:8). ^{1}H NMR (500 MHz, MeOD): δ = 6.13 (dd, 1H, J = 1.0 Hz, J = 1.5 Hz), 5.65 (t, 1H, J = 1.5 Hz), 4.83 (d, 1H, J = 1.5 Hz), 4.35 (ddd, 1H, J = 3.0 Hz, J = 6.0 Hz, J = 12.0 Hz), 4.32 (ddd, 1H, J = 3.0 Hz, J = 6.0 Hz, J = 12.0 Hz), 3.96 (ddd, 1H, J = 3.0 Hz, J = 6.0 Hz, J = 11.5 Hz), 3.81−3.84 (m, 2H), 3.74 (ddd, 1H, J = 2.5 Hz, J = 6.0 Hz, J = 11.5 Hz), 3.73 (t, 1H, J = 5.5 Hz), 3.69 (dd, 1H, J = 3.5 Hz, J = 10.0 Hz), 3.64 (t, 1H, J = 9.5 Hz), 3.55−3.59 (m, 1H), 1.95 (s, 3H) ppm. ^{13}C NMR (100 MHz, $CDCl_3$): δ = 167.3, 136.2, 125.0, 100.2, 73.3, 71.1, 70.7, 67.0, 64.9, 63.4, 61.4, 17.0. IR (neat): $\tilde{\nu}$ = 3375, 2920, 1711, 1634, 1453 cm^{-1}. HRMS (ESI): calcd for $C_{12}H_{20}O_8NH_4$ $[M + NH_4]^+$ 310.1502; found 310.1494.

^{1}H and ^{13}C NMR spectra of all the compounds (**1**−**5**) are presented in Supporting Information Figures S1−S10.

Synthesis of RAFT-Modified Silica Nanoparticles (SiNP-CPDB). Grafting of RAFT to the SiNP surface was carried out in multiple steps as shown in Scheme 2.[42] In the first step, synthesized SiNP was modified with amine functionality (SiNP-NH_2) which on further reaction with activated RAFT agent produced RAFT-modified SiNP. RAFT agent 4-cyanopentanoic acid dithiobenzoate (CPDB) was activated using *N*-hydroxysuccinamide (NHS) to obtain activated CPDB which is named as CPDB-NHS. The detailed procedure for the preparation and activation of RAFT agent, synthesis of silica particles, and amine modification of silica are presented in the Supporting Information. SiNP-NH_2 (2.75 g) was dispersed in dry THF (70 mL) and ultrasonication for 30 min followed by nitrogen purging for 20 min while stirring. To this, activated CPDB (CPDB-NHS, 0.5 g, 1.3 mmol) was added under stirring, and the mixture was stirred for 24 h at room temperature. After the reaction, the reaction mixture was precipitated from 4:1 mixture of cyclohexane and diethyl ether (400 mL) and isolated by using centrifugation at 8000 rpm for 20 min. This purification cycle was repeated three times, and the obtained RAFT-functionalized silica nanoparticles (SiNP-CPDB) were dried under vacuum at 50 °C for 48 h. The yield obtained was 2.45 g (89%). The whole process of SiNP-CPDB synthesis is shown in Scheme 2.

Polymerization of MEMA Using SiNP-CPDB. We have carried out the polymerizations in two different solvents, namely a mixture of water:ethanol (7:3) and DMF, to check the suitability of solvent so as to get a good amount of glycopolymer (GP) loading on the SiNP surface. We have also executed many control reactions to check the role of free CPDB (RAFT agent) in the reaction mixture.

Water-Based Reactions. Into a series of Schlenk tubes containing a 7:3 mixture of water and ethanol (1.4 mL), SiNP-CPDB (0.1 g, which has 7.607 μmol of CPDB), MEMA (calculated amount, we have varied this amount to obtain different chain lengths), $NaHCO_3$ (2 mg), free CPDB (2.13 mg, 7.607 μmol), and ACP (0.426 mg, 1.521 μmol) were added by keeping the ratio of [SiNP-CPDB]:[free CPDB]:[ACP] = 1:1:0.2 constant for all the reactions; only the amount of MEMA was altered. These reaction vials were then sealed and subjected to three freeze−pump−thaw cycles followed by sonication for 10 min and stirred for 16 h in a preheated oil bath at 70 °C. After completion of the reaction, the reaction mixture was quenched using liquid nitrogen. The glycopolymer-grafted silica nanoparticles (GP-*g*-SiNP) were precipitated from a large excess of hexane and isolated by using centrifugation at 7000 rpm for 30 min. The precipitate obtained was redispersed in methanol (40 mL) and centrifuged at 7000 rpm for 30 min. This step was repeated thrice, and the obtained GP-*g*-SiNP was dried under vacuum at 70 °C for 48 h. We have altered the amount of glycomonomer (MEMA) in the reaction medium by keeping all the other reagents constant so as to obtain different chain length of GP poly(MEMA) chain on the SiNP surface.

DMF-Based Reactions. The polymerization reactions were also conducted using the identical protocols as described above in DMF solvent.

Homopolymerization of MEMA Monomer Using CPDB as RAFT Agent. In a 10 mL Schlenk tube containing DMF (3 mL), MEMA (300 mg, 1.0273 mmol), CPDB (4.189 mg, 15 μmol), and ACP (0.42 mg, 1.5 μmol) were added. The reaction tube was sealed and subjected to three freeze−thaw cycles followed by sonication for 10 min and stirred for 16 h in a preheated oil bath at 70 °C. The reaction mixture was subsequently quenched using liquid nitrogen; the GP was precipitated from a large excess of cold hexane/diethyl ether mixture and isolated by filtration. This precipitation step was repeated twice, and the obtained GP was dried under vacuum at 60 °C for 24 h.

Cleaving of the GP Chains from the GP-*g*-SiNP. The GP was cleaved from the GP-*g*-SiNP according to the procedure described elsewhere.[42,43] Briefly, the process is as follows: in a polyethylene tube, the GP-*g*-SiNP (30 mg) was dissolved in 6 mL of DMF. Aqueous hydrofluoric acid (HF, 48 wt %, 0.6 mL) was added to this solution, and the reaction mixture was stirred at room temperature for 6 h. The polymer was precipitated by adding the polymer solution into 20-fold of excess cold hexane/diethyl ether mixture in a polyethylene beaker, and the precipitate was collected by filtration. The GP obtained was dried in a vacuum oven at 80 °C for 24 h. The recovered GP chains were then subjected to molecular weight analysis and protein binding studies as glycopolymer without any SiNP.

Characterization Techniques. All the details of various characterization techniques which were used to characterize GP-*g*-SiNP are presented in the Supporting Information.

Interaction of GP-*g*-SiNP with Con A: ITC Studies. Con A was purified from jack beans (*Canavalia ensiformis*) as described earlier.[44,45] A VP-ITC isothermal titration calorimeter from MicroCal (Northampton, MA) equipped with a 1.445 mL sample cell was used for all

DOI: 10.1021/acs.macromol.7b01265
Macromolecules XXXX, XXX, XXX−XXX

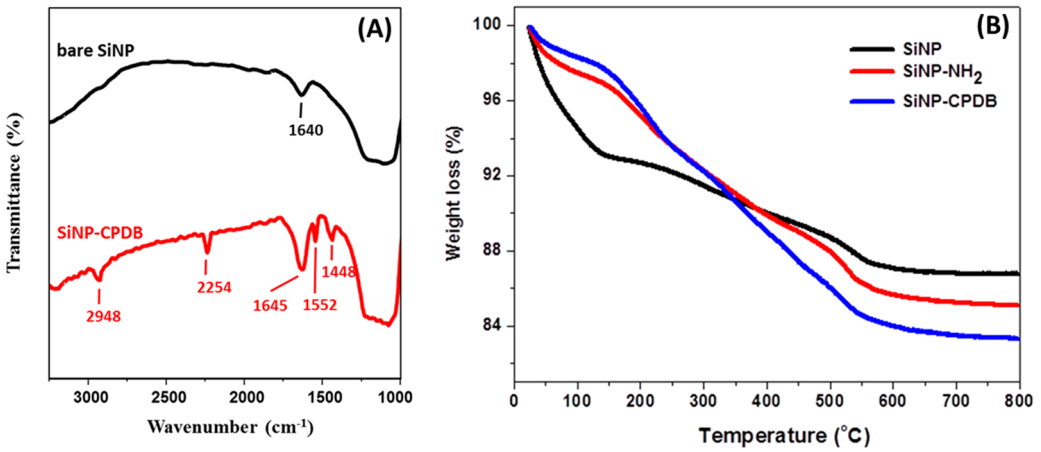

Figure 1. FT-IR spectra (A) and TGA profiles (B) of bare SiNPs and RAFT-modified SiNPs.

the experiments. Before titrations Con A samples were dialyzed extensively against 10 mM Tris buffer, pH 7.6, containing 0.15 M NaCl, 1 mM $CaCl_2$, and 1 mM $MnCl_2$ (TBS) and degassed properly using a ThemoVac degassing unit. The GP-*g*-SiNP and the glycopolymer (GP chains after removal of SiNP by HF treatment as described in the previous section) solutions were prepared in TBS buffer. Calorimetric titrations were carried out essentially as described previously[46] with minor modification. Briefly, 7 μL aliquots of 5 mM glycopolymer solution were added to a 100 μM Con A (monomer concentration) solution taken in the sample cell at 7 min intervals via a rotating stirrer−syringe. For investigating GP-*g*-SiNP-Con A interaction, titrations were performed by injecting 8 μL aliquots of 1 mM Con A (monomer concentration) into 2.5 mM GP-*g*-SiNP solution taken in the cell. A blank titration in each case was carried out in order to estimate heat changes arising due to ligand−buffer interactions, and the resulting heat changes were subtracted from the changes observed in the main titration. The titration data could be analyzed satisfactorily by MicroCal Origin ITC software using "one set of sites" binding model as described elsewhere,[46,47] which yielded the following thermodynamic parameters associated with the binding reaction: association constant (K_a), binding stoichiometry (n), and enthalpy of binding (ΔH). After that free energy (ΔG) and entropy (ΔS) of binding were calculated according to the following equations:

$$\Delta G = -RT \ln K_a \quad (1)$$

$$\Delta G = \Delta H - T\Delta S \quad (2)$$

RESULTS AND DISCUSSION

Polymerizable SiNP Surface. In this article, we report the successful grafting of mannose-based glycopolymers (GP) on silica nanoparticles (SiNP) surface using the *grafting-from* RAFT polymerization technique. A multistep process has been developed to prepare glycopolymer-grafted SiNP (GP-*g*-SiNP). First, the well-known Stöber method was followed to prepare monodisperse SiNPs from tetraethyl orthosilicate [$Si(OEt)_4$] through a hydrolysis and condensation reaction.[48] The measured particle size obtained from FE-SEM and TEM is 47 ± 2 nm in diameter as shown in Figure S11, and the particle size measured using light scattering (Figure S12) is 54 nm. These particles are highly monodisperse, and the size of these nanoparticles can be readily controlled by altering the mole ratio of the reactants used in the synthesis. In the second step of GP-*g*-SiNP preparation, the amine-functionalized silica nanoparticles (SiNP-NH_2) were prepared by refluxing (3-aminopropyl)triethoxysilane (APTES) with silica nanoparticles (SiNP) as shown in Scheme 2, and the measured particle size of SiNP-NH_2 is 47 ± 2 nm (FESEM and TEM Figure S1I) and 65 nm (light scattering, Figure S12).

It is well-known that dithiobenzoate-based RAFT agents can control the radical polymerization of a wide range of monomers including methacrylates, acrylates, styrene, etc.,[49,50] to provide polymers with predictable molecular weight and narrow polydispersities. The carboxylic functionality of RAFT agent CPDB can be readily utilized to immobilize CPDB on particle surface through a covalent amide bond with SiNP-NH_2. Accordingly, in the third step of GP-*g*-SiNP preparation, *N*-hydroxysuccinamide (NHS) activated CPDB (CPDB-NHS), as shown in Scheme 2, was successfully attached to silica nanoparticles by reacting with amine-modified SiNP (SiNP-NH_2).[42,51] The FESEM and TEM images of CPDB-modified silica nanoparticles (SiNP-CPDB) are presented in Figure S11 along with bare SiNP and SiNP-NH_2. The measured particle size is 48 ± 3 nm (FESEM and TEM, Figure S11) and 59 nm (light scattering, Figure S12).

FT-IR and TGA analyses provide clear evidence for the step-by-step surface modification of SiNPs. Figure 1A compares the FT-IR spectra of the SiNP-CPDB with the bare SiNP. The sharp bands at 1645 and 1552 cm^{-1} are due to C═O and N−H stretching of amide group, respectively. The IR band at 2254 cm^{-1} is due to the C≡N stretching frequency of CPDB, and peaks at 2948 and 1448 cm^{-1} appear because of the saturated C−H vibrations of CPDB. This indicates that the dithiobenzoate group of CPDB RAFT agent is covalently attached to the surface of the SiNPs. The TGA profiles shown in Figure 1B display that the final weight loss increases from bare SiNP to SiNP-NH_2 to SiNP-CPDB due to the attachment of organic groups (propylamine or CPDB) to the surface of the SiNPs. The amount of RAFT agent (CPDB) which is covalently attached to the SiNPs was calculated from the TGA plots and found to be equal to 21.3 mg/g (76 μmol/g).[30,52] The calculated RAFT agent (CPDB) surface density from the loaded amount of CPDB on the 48 nm SiNP particles is found to be equal to 1.798 RAFT agents/nm^2. ^{13}C NMR (Figure S12) also gives the clear evidence of the successful surface grafting of CPDB. The peaks at 168, 144, and 120 ppm are due to the amide carbonyl carbon, anomeric carbon of phenyl ring in CPDB, and the cyano group in CPDB, respectively. The peaks around 124−130 ppm and between 18 and 40 ppm are due to the phenyl ring carbon atoms and the alkyl carbons from CPDB RAFT agent and SiNP-NH_2, respectively.

DOI: 10.1021/acs.macromol.7b01265
Macromolecules XXXX, XXX, XXX−XXX

Scheme 3. Synthesis of GP (pMEMA)-Grafted SiNPs (PMEMA-*g*-SiNP) from RAFT-Modified Polymerizable SiNP

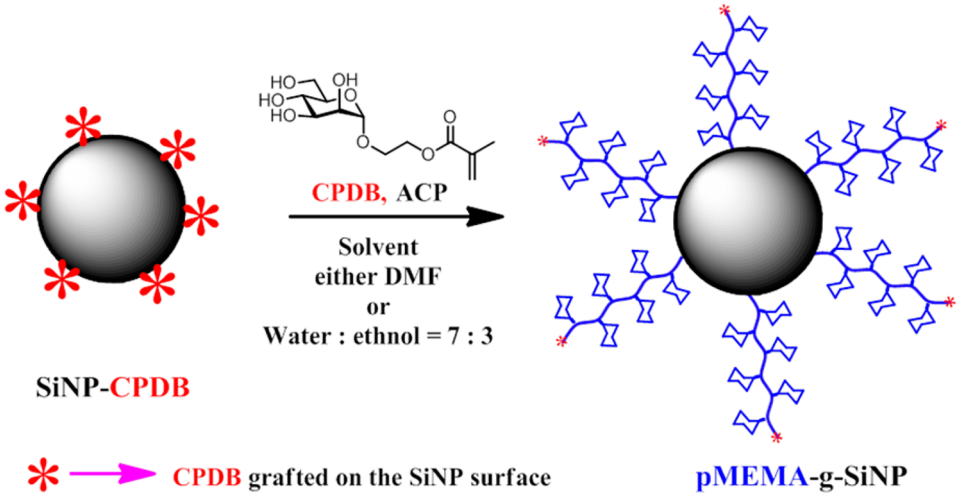

Table 1. Summary of Various Physical Data of pMEMA-*g*-SiNP[a]

sample identity	sample type	amount of GP grafting (wt %/GP-*g*-SiNP)[b]	targeted $\bar{M}_n$[c]	$\bar{M}_n$[d]	PDI[d]	size (TEM) (nm)[e]	size (light scattering) (nm)[f]
	SiNP-CPDB					48	58
P1	$pMEMA_{18}$-*g*-SiNP	2.7	5000	5500	1.22	49	105
P2	$pMEMA_{24}$-*g*-SiNP	4.2	10000	7100	1.19	50	122
P3[g]	$pMEMA_{16}$-*g*-SiNP	2.8	10000	4900	1.19	49	117
P4	$pMEMA_{9}$-*g*-SiNP	9.5	2500	2700	1.17	51	91
P5	$pMEMA_{32}$-*g*-SiNP	19.4	10000	9400	1.19	53	141
P6	$pMEMA_{138}$-*g*-SiNP	38.1	50000	40400	1.37	57	164
P7	$pMEMA_{74}$ (GP)		20000	21700	1.06		

[a]The polymerization of MEMA was carried out in two different solvents: **P1**, **P2**, and **P3** are carried out in a water/ethanol (7:3) mixture, 2 mg of $NaHCO_3$ is added to dissolve ACP initiator, and **P4**–**P7** are carried out in dry DMF. [b]Estimated from the TGA analysis. [c]Targeted $\bar{M}_n$ is calculated based on the equation which is generally used for RAFT polymerization. [d]Determined by gel permeation chromatography. [e]With a standard deviation of ±2 until **P4** and ±4 for **P5** and **P6**. [f]Measured in water medium, and size polydispersity obtained from light scattering is less than 0.1. [g]Reaction was carried out without the addition of free CPDB.

The particle size and size distribution of SiNPs were measured in water by light scattering measurements, and the results obtained are presented in Figure S12B. The mean diameter of bare SiNP is 53 nm and increased to 64 nm upon the amine modification which is due to the formation of hydrophilic amine shell and then decreased to 58 nm after attaching CPDB on SiNP particle surface. The decrease in the diameter may be due to a decrease in hydration shell of the particle after CPDB attachment owing to the hydrophobic nature of attached CPDB. Hence, the above discussions clearly prove that the SiNP surface is now ready for further grafting of polymer (glycopolymer) chain.

Growth of Mannose-Based Glycopolymer Chain on the SiNP Surface. Polymer chains can be grown on any solid (particle) surface using the RAFT-mediated *grafting-from* approach. There are two methods, namely "arm-first" and "core-first", by which polymer chain be grown using the *grafting-from* RAFT method.[39,53,54] The relatively lower grafting density on the particle surface is usually achieved in the arm-first way,[39] where the Z-group of the RAFT agent is attached to the particle surface whereas the R-group of the RAFT agent is attached to the particle surface in the case of the "core-first" method. The SiNP-CPDB has an R-group on the SiNP surface; therefore, any growth of chain in the current surface is expected to yield higher grafting density of the polymer chain.

The MEMA monomer was synthesized using the protocol described in the Experimental Section (Scheme 1) in multiple steps. All the characterization data are also included in the Experimental Section. The ^1H and ^{13}C NMR spectra of all the compounds synthesized in each step are presented in Supporting Information (Figures S1–S10), and the data confirm the structure of MEMA. The polymerizable SiNP-CPDB surface is used to grow the poly(mannosyloxyethyl methacrylate) (pMEMA) chain to produce the GP-*g*-SiNP where GP is pMEMA, and hence this point onward we refer to it as pMEMA-*g*-SiNP. The reaction scheme for the pMEMA grafting is pictorially presented in Scheme 3. The polymerization was carried out in two different solvents: water/ethanol mixture (7:3) and DMF. The polymerization of MEMA in the presence of SiNP-CPDB was performed using an additional amount of CPDB as a free chain transfer agent and ACP as a thermal initiator at 70 °C by keeping the reactant ratio as [SiNP-CPDB]:[free CPDB]:[ACP] = 1:1:0.2, and this ratio was kept constant for various sets of the reaction while varying the amount of MEMA to get different chain lengths of pMEMA on the SiNP surface. Table 1 summarizes physical details of all the synthesized polymers. To check the suitability of solvents, we have synthesized a series of polymers with variable chain lengths of pMEMA, and this has been achieved by varying the feed of MEMA monomer in the polymerization. **P1**, **P2**, and **P3** samples (refer Table 1) were obtained in the water/ethanol

DOI: 10.1021/acs.macromol.7b01265
Macromolecules XXXX, XXX, XXX–XXX

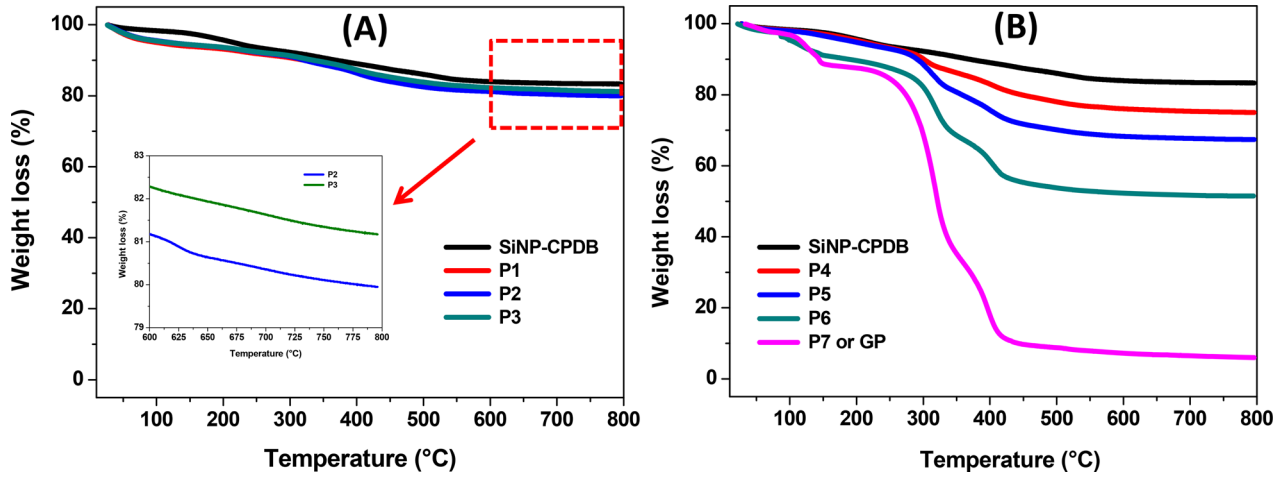

Figure 2. TGA analysis of pMEMA-*g*-SiNP samples of different chain lengths obtained from two different solvents: water/ethanol (A) and DMF (B). Inset shows the difference in weight loss in the case of **P2** and **P3**.

(7:3) mixture, and **P4**, **P5**, and **P6** (refer Table 1) were obtained using DMF as the solvent. **P7** is also obtained using DMF solvent without any SiNP core. The number of repeat units (as presented in the subscript of sample type in Table 1) is calculated from the molecular weight data which is obtained from GPC measurement and will be discussed in detail in a later section.

The relative amount of pMEMA (GP) grafted to SiNPs in the final products can be estimated from the TGA results. Figure 2 shows the TGA curves for the SiNP-CPDB and SiNPs-*g*-pMEMA-*g*-SiNP prepared using two different solvents and pMEMA (homopolymer without grafting on to the SiNP surface). The decomposition temperature range for all the samples is 250−600 °C as shown in Figure 2. The pure pMEMA (without SiNP, **P7**) decomposed completely as can be seen from the TGA graphs (Figure 2B). The TGA data clearly show that with increase in pMEMA chain length (refer to Table 1) the final weight loss increases (**P4** to **P6** weight loss increases significantly), which in turn attributes a higher amount of GP loading on the SiNP surface. Similarly, a comparison of **P2** and **P3** GPC data (Table 1) confirms the higher chain length of **P2** than **P3**, which is also proved from the higher weight loss in the case of **P2** as shown in the inset of Figure 2A.

The above discussion clearly demonstrated that we were able to control and alter the pMEMA chain length on the SiNP surface by choosing the appropriate reaction recipe. However, it must be noted that the number of pMEMA chains grafted on the SiNP surface (can be called as grafting density) remains identical for all the pMEMA-*g*-SiNP samples since we have used the same surface-activated SiNPs (SiNP-CPDB) for carrying out all the polymerization. The growth of pMEMA chains starts from the CPDB, and therefore the grafting density can be altered only by changing the amount of CPDB loaded on the SiNP surface. The variation of grafting density on the SiNP surface may influence the lectin binding properties of this class of materials, and further investigation on this aspect is in progress in our laboratory.

Role of Solvent and Free RAFT Agent in the Polymerization. We have carried out the polymerization in two different solvents to check the role of solvent in the polymerization of MEMA in the *grafting-from* RAFT approach. Similar reactions (**P2** and **P5**) in two different solvents (water/ethanol mixture and DMF) and identical targeted molecular weight (10 000 g/mol) by keeping all other reaction conditions unchanged were conducted. The relative amount of GP that is grafted to SiNP is analyzed from the TGA data (Figure S13). As seen from the TGA graph (Figure S13), the final weight loss is significantly higher when the polymer is prepared from DMF solvent (**P5**) than in water solvent (**P2**), and this clearly indicates the growth of bigger chain in the case of DMF than aqueous solvent. This may be due to the higher reinitiating capacity of the formed oligomeric radicals in DMF compared to water solvent. The calculated loading presented in Table 1 also proves higher GP loading in the case of **P5** than **P2**. Although the targeted molecular weight for both **P5** and **P2** is 10 000 g/mol, the measured (using GPC) $\bar{M}_n$ values of **P5** is higher than **P2**, which also confirms that the DMF is better than the aqueous solvent. Therefore, we can conclude that DMF is a better solvent for MEMA polymerization and results in the grafting of higher amount of pMEMA on the SiNP surface.

Further, we want to check the role of free CPDB (RAFT agent) in the polymerization of MEMA using the *grafting-from* RAFT approach. For this reason, we have conducted a set of same reactions with identical targeted MW (**P2** and **P3**, details are presented in Table 1) where we have taken all the ingredients in the same proportion except that free CPDB is not added in the case of **P3** and to maintain the [M]:[R]:[I] ratio, we have also halved the monomer as well as initiator in the case of **P3**. The TGA data of isolated **P2** and **P3** samples (inset of Figure 2A) clearly show less weight loss in the case of **P3** compared to **P2**. This is attributed to the higher grafting of pMEMA on SiNP in the presence of free CPDB as also can be verified from the GP grafting amount (calculated from TGA) as shown in Table 1. The excess CPDB in the polymerization mixture helps in exchanging oligomeric radicals, and therefore the polymerization goes more steady which leads to high GP grafting. Hence, we have conducted remaining reactions (**P4**−**P6**) with the addition of a similar amount of free CPDB and in DMF so that we can achieve better GP grafting.

Spectroscopic Evidence of Poly(MEMA) Grafting on SiNP. The grafting of pMEMA on the particle surfaces is confirmed by comparing the FT-IR spectra of SiNP-CPDB, pMEMA-*g*-SiNP, and pMEMA (Figure 3). The spectrum of pMEMA-grafted SiNP shows a peak at around 1217 cm^{-1} which corresponds to C−O bond stretching of the mannose

DOI: 10.1021/acs.macromol.7b01265
Macromolecules XXXX, XXX, XXX−XXX

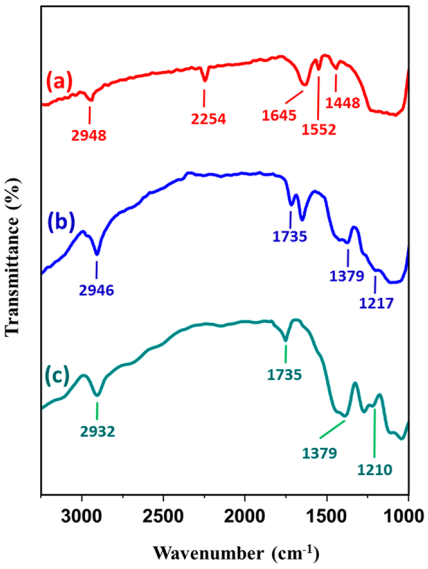

Figure 3. FT-IR spectra of (a) SiNP-CPDB, (b) pMEMA-*g*-SiNP, and (c) pMEMA.

moiety, which is apparent in the pMEMA spectrum at 1210 cm^{-1}. The bands observed at 1379 and 1735 cm^{-1} are assigned to the C−O−C group and C═O ester double bond of the mannose sugar, respectively, and these are also seen in pMEMA. The presence of characteristic bands of SiNP-CPDB on the pMEMA-*g*-SiNP spectrum proves that pMEMA is grafted on the SiNP-CPDB surface.

The grafting of GP on SiNP surface was further confirmed by ^{13}C NMR spectroscopy. Figure 4 represents the ^{13}C NMR spectra of GP-*g*-SiNP recorded in D_2O solvent. A peak at 170.9 ppm corresponds to the carbonyl carbon (C═O) of the ester from the pMEMA. The peak at 105.8 ppm is due to the anomeric carbon of mannose in MEMA. Several peaks between 64 and 77 ppm are attributed to the five remaining carbons from the mannose ring, and the remaining two peaks are due to the ethylene part of MEMA. Two peaks at 48.6 and 29.2 ppm are assigned to the polymer backbone, indicating the successful grafting of pMEMA on the SiNP nanoparticle surface.

Particle Size and Dispersity. Figure 5 and Figure S14 show the FE-SEM and TEM images of pMEMA-*g*-SiNP prepared from both DMF and water/ethanol solvents. In an earlier section, we have observed that the surface of SiNP-CPDB (Figure S11c) is smooth and without much roughness, but GP-*g*-SiNP samples show a rough surface (FESEM images) and also agglomeration of silica particles is seen as shown in TEM images (Figure 5, right panel). This observation is

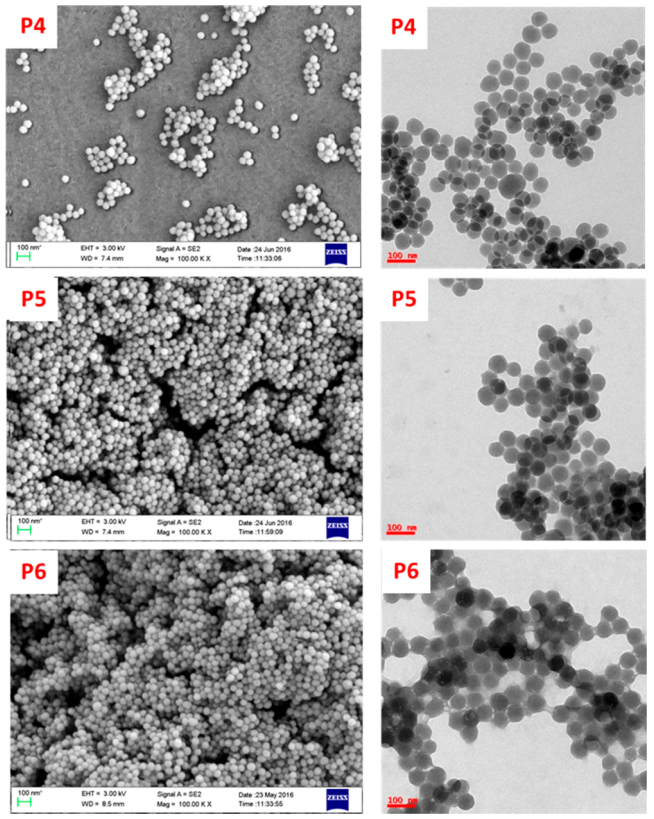

Figure 5. FE-SEM images (left panel) and TEM images (right panel) of pMEMA-*g*-SiNP nanoparticles obtained after purification for different chain lengths prepared using DMF as a solvent. The sample identification (**P4**, **P5**, and **P6**) can be found in Table 1.

attributed to the presence of pMEMA on the surface of SiNP. The increase in particle agglomeration with increase in chain length of the grafted pMEMA nanoparticles when compared with SiNP-CPDB (Figure.S11c) is very clear in all the cases as shown in Figure 5 and Figure S14. This kind of crowding of particles may be due to the interaction between the pMEMA chain within the particle and with the neighboring particles. The increase in particle size (Table 1) from 48 ± 2 nm (SiNP-CPDB) to 57 ± 4 nm (**P6**) after grafting the pMEMA chains reveals that the chains are chemically bound to the silica nanoparticles. FE-SEM and TEM analyses of the SiNP before and after grafting show that the shape and size distribution of the particles remain unchanged, indicating that the nanoparticles are stable under the current polymerization conditions.

The particle size and size distribution of pMEMA-*g*-SiNP samples were also estimated in water by light scattering

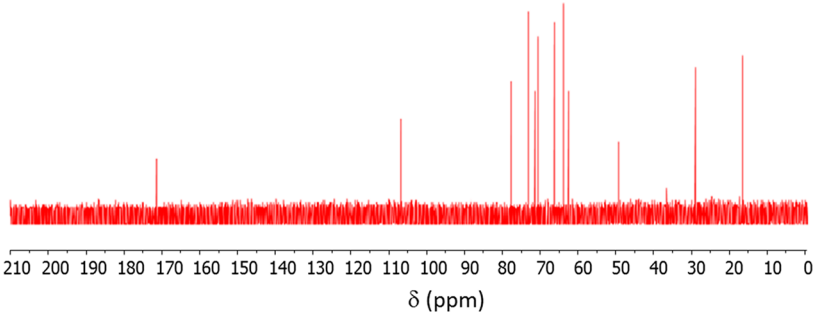

Figure 4. ^{13}C NMR spectrum of pMEMA-*g*-SiNP. Spectrum was recorded in D_2O by dispersing the solid particles of the sample.

DOI: 10.1021/acs.macromol.7b01265
Macromolecules XXXX, XXX, XXX−XXX

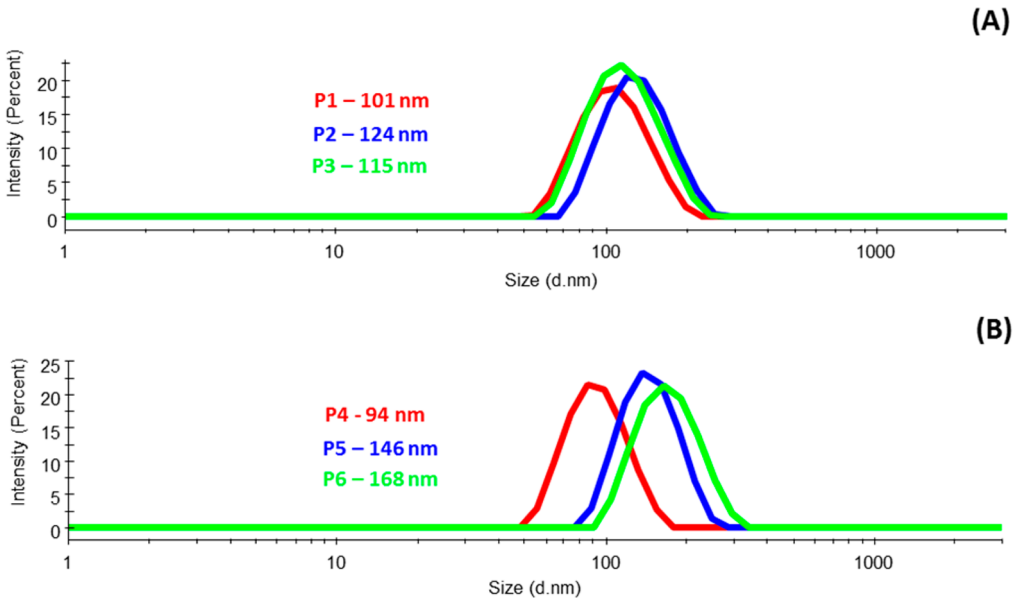

Figure 6. Light scattering results of pMEMA-*g*-SiNP obtained from the polymerization conducted in (A) water/ethanol (7:3) and (B) DMF solvents.

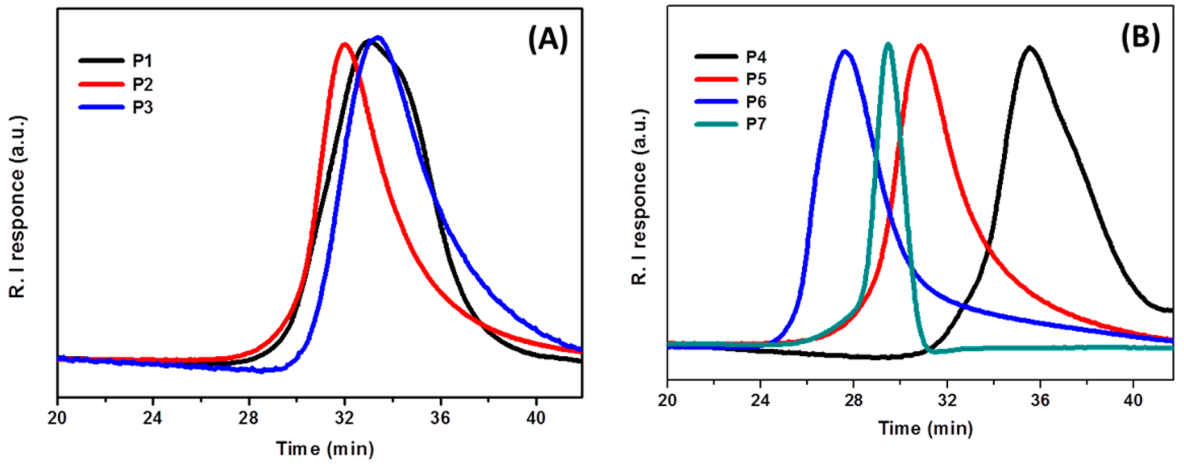

Figure 7. GPC curves of pMEMA chains cleaved from pMEMA-*g*-SiNP by using aqueous HF. Polymers obtained using water/ethanol (A) and DMF (B) as a solvent for the polymerization.

measurements (Figure 6), and the results obtained are listed in Table 1. Even though the core (SiNP-CPDB) diameters of all the particles are the same (as prepared from the same sample of SiNP-CPDB), the hydrodynamic diameter of pMEMA-*g*-SiNP has increased by 2−3-fold (Table 1), indicating that the pMEMA-*g*-SiNP possesses the graft pMEMA chains which are highly hydrophilic and are in the swollen state. The size from light scattering measurement is proportional to the GP chain length on the particle surface; in other words, the particle size increases with increasing chain length of pMEMA (Table 1). The core reason for this increase in the hydrodynamic diameter is a result of the surface grafting of pMEMA chains on SiNP, and similar results are obtained by others when particles are coated with a hydrophilic polymer chain.[55] These results indicate that the grafting of pMEMA on the SiNP surface was successfully achieved by RAFT-mediated controlled radical polymerization of MEMA using SiNP-CPDB. A comparison of size measured from microscopic and light scattering techniques reveals that pMEMA chain is in the swollen state in the solvent but in collapsed state in dry conditions. It must be noted from the data presented in Table 1 that the changes in particle size are almost insignificant with increasing GP chain length in the case of data obtained from the microscope technique; however, it is a very significant increase with increasing GP chain length when measured in an aqueous medium. This observation once again reiterates the swelling nature of the hydrophilic pMEMA chain. It should be mentioned that all the particles are highly monodisperse in nature as seen from both microscopic and light scattering data.

Molecular Weight of Grafted pMEMA on SiNP Surface. The molecular weight and molecular weight distributions of grafted polymer chains, the pMEMA chains, were measured using GPC after cleaving the polymer from SiNP by treating the pMEMA-*g*-SiNP with aqueous HF solution. Figure 7 shows the GPC chromatograms of all the samples which are obtained after cleaving from SiNP surface. The GPC curves are all symmetric, unimodal, and narrow, attributing that the polymerization proceeded in a controlled manner. The number-average molecular weight ($\bar{M}_n$), poly-dispersity index (PDI), and the number of pMEMA chain

DOI: 10.1021/acs.macromol.7b01265
Macromolecules XXXX, XXX, XXX−XXX

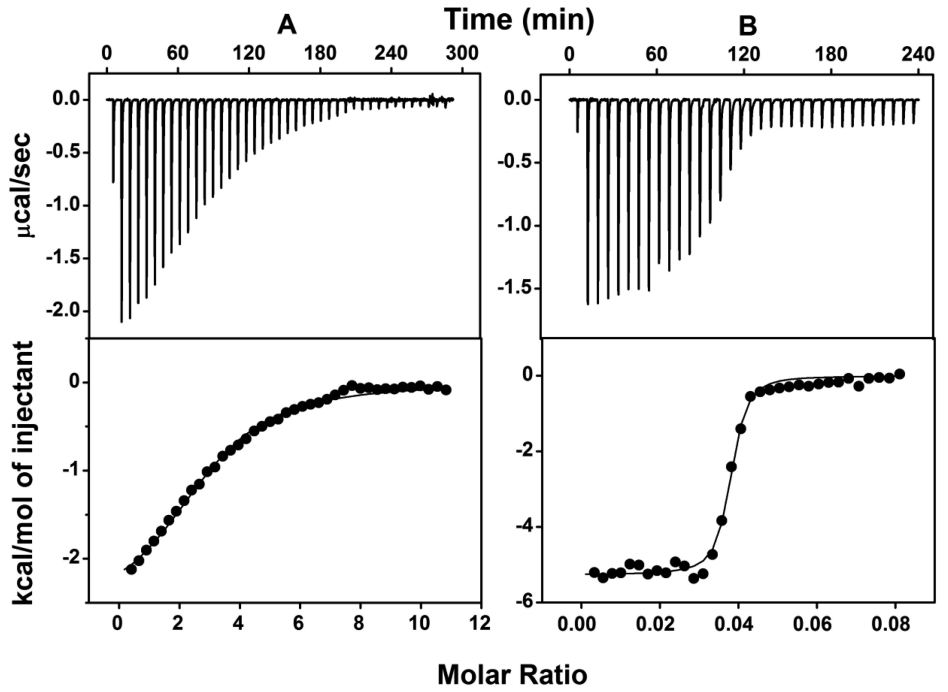

Figure 8. Calorimetric titration of Con A with (A) **P7** [pMEMA$_{74}$ (GP)] and (B) **P5** [pMEMA$_{32}$-*g*-SiNP] at 25 °C. Upper panel of A displays the raw ITC data obtained from 40 automatic injections of 7 μL aliquots of 5 mM **P7** into 100 μM Con A while upper panel of B displays 35 automatic injections of 8 μL aliquots of 1 mM Con A into 2.5 mM **P5**. Lower panels show the integrated data obtained from the raw data shown in the upper panels.

Table 2. Binding Constants (K_a), Stoichiometry (n), Binding Enthalpy (ΔH), and Entropy (ΔS) for the Interaction of Con A with pMEMA$_{74}$ (GP) and pMEMA$_{32}$-*g*-SiNP Obtained from "One Set of Sites" Binding Model[a]

sample	n	K_a (M^{-1})	ΔH (kcal mol^{-1})	ΔS (cal mol^{-1} K^{-1})
MeαMan	1.0	$(7.0 \pm 0.3) \times 10^3$	-6.3 ± 1.4	-3.6 ± 4.5
P7 [pMEMA$_{74}$ (GP)]	2.79 ± 0.13	$(1.45 \pm 0.05) \times 10^4$	-2.7 ± 0.1	9.9 ± 0.2
P5 [pMEMA$_{32}$-*g*-SiNP]	30.19 ± 3.24	$(5.77 \pm 1.99) \times 10^6$	-5.2 ± 0.1	13.5 ± 1.1

[a]Data for MeαMan binding were taken from ref 56.

(calculated from $\bar{M}_n$) of all the polymers are tabulated in Table 1. The narrow PDI values (<1.4) indicated that the polymerization proceeded in accordance with a controlled/living radical polymerization mechanism as expected from RAFT method. The number-average degree of polymerization (DP) is calculated from $\bar{M}_n$ and presented in Table 1 with the sample identification. It must be noted that the $\bar{M}_n$ obtained from GPC is in excellent agreement with the $\bar{M}_n$ (Table 1) values theoretically calculated from monomer and RAFT agent concentration in the polymerization feed. This indicates a high degree of conversion and well-controlled reaction. Another interesting observation from Table 1 and Figure 7A is the $\bar{M}_n$ value of **P3**. The calculated $\bar{M}_n$ (targeted) at **P3** is 10 000 g/mol; however, $\bar{M}_n$ from GPC is only 4900 g/mol. This is simply because of the absence of free RAFT agent. This once again reconfirms the necessity of addition of free RAFT agent (CPDB) in the polymerization feed.

Interaction of pMEMA-*g*-SiNP and pMEMA with Con A. Results of calorimetric titrations between the mannose-specific lectin, Con A, and pMEMA-*g*-SiNP as well as pMEMA are shown in Figure 8. The upper panels represent the exothermic heat of binding at each injection which gradually decreases until saturation is achieved. The lower panels represent plots of incremental heat released as a function of glycopolymer/Con A monomer ratio where nonlinear least-squares fit of the data to "one set of sites" model are shown as solid lines. The close agreement of the solid lines with the experimental data indicates that the binding model satisfactorily fits the data for pMEMA as well as pMEMA-*g*-SiNP. All the experiments were performed in duplicate, and the average thermodynamic parameters obtained by analyzing the raw data are listed in Table 2. For comparison, corresponding values for the binding of methyl-α-D-mannopyranoside (MeαMan), taken from the literature,[56] are also listed in Table 2.

The glycopolymer (pMEMA) **P7** with 74 mannose residues per chain shows a stoichiometry close to three (2.79 ± 0.13) for its binding to Con A, indicating that approximately one mannose residue out of three residues binds to a Con A subunit. The association constant obtained for this binding (1.45×10^4 M^{-1}) is about 2-fold higher than the value reported for the Con A−MeαMan interaction.[56] On the other hand, the grafted glycopolymer on SiNP (pMEMA$_{32}$-*g*-SiNP, **P5**) bearing 32 mannose residues exhibits a stoichiometry of 30 for its binding to Con A. It indicates that only one mannose residue per chain can bind to Con A, but with a much higher affinity. The association constant for this interaction is 5.77×10^6 M^{-1}, which is ~400-fold higher than that obtained for the interaction between the glycopolymer (**P7**) and Con A.

It is instructive to compare the thermodynamic parameters obtained for the binding of the glycopolymer **P7** and the

DOI: 10.1021/acs.macromol.7b01265
Macromolecules XXXX, XXX, XXX−XXX

glyconanoparticle (glycopolymer grafted on SiNP) **P5** with those reported for the monosaccharide MeαMan. It is interesting to note that while the enthalpy of binding for the association of MeαMan is higher than the values obtained for the binding of **P7** and **P5**, a negative contribution associated with the binding of MeαMan makes the overall binding weaker. On the other hand, although the enthalpy of binding associated with the glycopolymer is less than half of that for the monosaccharide, a positive entropic contribution (ΔS = 9.9 cal mol^{-1} K^{-1}) associated with its binding results in the K_a value for **P7** being 2-fold higher. Finally, for the glyconanoparticle **P5** interaction with Con A, although the enthalpy of binding is marginally smaller than that for MeαMan, due to the relatively larger positive binding entropy makes its binding ~800- and 400-fold stronger than MeαMan and **P7**, respectively. The positive entropic contribution for the binding of Con A to **P5** and **P7** may be attributed to the increased statistical probability of the binding of the lectin to the GP and GP-*g*-SiNPs due to the proximal presence of multiple mannose moieties in the neighborhood.

CONCLUSION

In summary, we have demonstrated a simple method to covalently graft glycopolymers (carbohydrates) on the surface of silica nanoparticles. Initially, CPDB RAFT agent anchored SiNPs were prepared, and then a mannose-containing glycopolymer chain was grown on the surface of SiNPs using the *grafting-from* RAFT polymerization method. The chain length of the GP on the SiNPs surface has been varied in order to graft higher amount of GP. The resulting GP-*g*-SiNP particles display a narrow size distributions and the size of the GP chain on the particle surface can be readily controlled by changing the monomer amount in the polymerization feed. Molecular weights obtained from GPC analysis after cleaving the GP from the SiNP confirm the formation of GP-*g*-SiNP. The microscopic, spectroscopic, thermal, and light scattering studies unequivocally confirm the formation of GP-*g*-SiNP particles. The mannose-containing GP-*g*-SiNP shows very strong binding affinity and selectivity toward lectin Con A. Currently, we are in the process of extending this method to graft multiple carbohydrates on the single nanoparticle surface and study the binding capability with various lectins. The present methodology delivers a controlled synthesis of well-defined core−shell nanoparticles with protein binding glycopolymer on the surface of the particles which may be useful for delivering new carbohydrate-based therapeutics.

ASSOCIATED CONTENT

Supporting Information

The Supporting Information is available free of charge on the ACS Publications website at DOI: 10.1021/acs.macromol.7b01265.

The mannose monomer synthesis step by step details and the ^{1}H and ^{13}C NMR spectra for the synthesis of sugar monomer (MEMA), details of SiNP synthesis, RAFT agent synthesis, RAFT agent modification/activation, grafting of RAFT on SiNP, all details of characterization techniques, FESEM, TEM, TGA, ^{13}C NMR, and light scattering data of bare SiNP, SiNP-NH$_2$, and SiNP-CPDB; FESEM and TEM data of pMEMA-*g*-SiNP nanoparticles prepared using water/ethanol solvent; TGA data of **P2** and **P5** polymers (PDF)

AUTHOR INFORMATION

Corresponding Authors

*Tel (91) 40 23134808; Fax (91) 40 23012460; e-mail tusharjana@uohyd.ac.in (T.J.).
*E-mail p_ramu_sridhar@uohyd.ac.in (R.S.P.).
*E-mail mjswamy@uohyd.ac.in (M.J.S.).

ORCID

S. N. Raju Kutcherlapati: 0000-0003-3958-9177
Tushar Jana: 0000-0002-3680-2959

Notes

The authors declare no competing financial interest.

ACKNOWLEDGMENTS

S.N.R.K. thanks the CSIR-SRF for fellowship. Authors also thank Mr. Durga Prasad for his cooperation with FESEM and TEM analysis. We thank Council of Scientific and Industrial Research (CSIR), Govt. of India, for the research funding through a research grant [02(0175)/14/EMR-II dated 07-05-2014]. Financial and infrastructure support from the University Grants Commission, New Delhi (through the UPE and CAS programs), and the Department of Science and Technology, New Delhi (through the PURSE and FIST programs), are gratefully acknowledged.

REFERENCES

(1) Sigal, G. B.; Mammen, M.; Dahmann, G.; Whitesides, G. M. Polyacrylamides bearing Pendant α-sialoside Groups Strongly Inhibit Agglutination of Erythrocytes by Influenza Virus: The Strong Inhibition Reflects Enhanced Binding through Cooperative Polyvalent Interactions. *J. Am. Chem. Soc.* **1996**, *118*, 3789−3800.

(2) Lee, Y. C.; Lee, R. T. Carbohydrate-Protein Interactions: Basis of Glycobiology. *Acc. Chem. Res.* **1995**, *28*, 321−327.

(3) Lundquist, J. J.; Toone, E. J. The Cluster Glycoside Effect. *Chem. Rev.* **2002**, *102*, 555−578.

(4) Sun, X.-L.; Cui, W.; Haller, C.; Chaikof, E. L. Site-Specific Multivalent Carbohydrate Labeling of Quantum Dots and Magnetic Beads. *ChemBioChem* **2004**, *5*, 1593−1596.

(5) Fasting, C.; Schalley, C. A.; Weber, M.; Seitz, O.; Hecht, S.; Koksch, B.; Dernedde, J.; Graf, C.; Knapp, E. W.; Haag, R. Multivalency as a Chemical Organization and Action Principle. *Angew. Chem., Int. Ed.* **2012**, *51*, 10472−10498.

(6) Reichardt, N.-C.; Martín-Lomas, M.; Penadés, S. Opportunities for glyconanomaterials in personalized medicine. *Chem. Commun.* **2016**, *52*, 13430−13439.

(7) Yilmaz, G.; Becer, C. R. Glyconanoparticles and Their Interactions with Lectins. *Polym. Chem.* **2015**, *6*, 5503−5514.

(8) Li, X.; Chen, G. Glycopolymer-based Nanoparticles: Synthesis and Application. *Polym. Chem.* **2015**, *6*, 1417−1430.

(9) Kirchner, C.; Liedl, T.; Kudera, S.; Pellegrino, T.; Muñoz Javier, A.; Gaub, H. E.; Stölzle, S.; Fertig, N.; Parak, W. J. Cytotoxicity of Colloidal CdSe and CdSe/ZnS Nanoparticles. *Nano Lett.* **2005**, *5*, 331−338.

(10) Wang, Q.; Bao, Y.; Ahire, J.; Chao, Y. Co-encapsulation of Biodegradable Nanoparticles with Silicon Quantum Dots and Quercetin for Monitored Delivery. *Adv. Healthcare Mater.* **2013**, *2*, 459−466.

(11) De, M.; Ghosh, P. S.; Rotello, V. M. Applications of Nanoparticles in Biology. *Adv. Mater.* **2008**, *20*, 4225−4241.

(12) Rosi, N. L.; Mirkin, C. A. Nanostructures in Biodiagnostics. *Chem. Rev.* **2005**, *105*, 1547−1562.

(13) Ahire, J. H.; Chambrier, I.; Mueller, A.; Bao, Y.; Chao, Y. Synthesis of D-Mannose Capped Silicon Nanoparticles and Their Interactions with MCF-7 Human Breast Cancerous Cells. *ACS Appl. Mater. Interfaces* **2013**, *5*, 7384−7391.

DOI: 10.1021/acs.macromol.7b01265
Macromolecules XXXX, XXX, XXX−XXX

(14) Kutcherlapati, S. N. R.; Yeole, N.; Gadi, M. R.; Perali, R. S.; Jana, T. RAFT Mediated One Pot Synthesis of Glycopolymer Particles with Tunable Core-Shell Morphology. *Polym. Chem.* **2017**, *8*, 1371−1380.
(15) Miura, Y.; Hoshino, Y.; Seto, H. Glycopolymer Nanobiotechnology. *Chem. Rev.* **2016**, *116*, 1673−1692.
(16) Li, Z.; Sun, L.; Zhang, Y.; Dove, A. P.; O'Reilly, R. K.; Chen, G. Shape Effect of Glyco-Nanoparticles on Macrophage Cellular Uptake and Immune Response. *ACS Macro Lett.* **2016**, *5*, 1059−1064.
(17) Basuki, J. S.; Esser, L.; Duong, H. T. T.; Zhang, Q.; Wilson, P.; Whittaker, M. R.; Haddleton, D. M.; Boyer, C.; Davis, T. P. Magnetic Nanoparticles with Diblock Glycopolymer Shells give Lectin Concentration-Dependent MRI Signals and Selective Cell Uptake. *Chemical Science* **2014**, *5*, 715−726.
(18) Kang, B.; Opatz, T.; Landfester, K.; Wurm, F. R. Carbohydrate Nano Carriers in Biomedical Applications: Functionalization and Construction. *Chem. Soc. Rev.* **2015**, *44*, 8301−8325.
(19) Chen, K.; Bao, M.; Bonilla, A. M.; Zhang, W.; Chen, G. A Biomimicking and Electrostatic Self-assembly Strategy for the Preparation of Glycopolymer Decorated Photoactive Nanoparticles. *Polym. Chem.* **2016**, *7*, 2565−2572.
(20) Muñoz-Bonilla, A.; Fernández-García, M. Glycopolymeric Materials for Advanced Applications. *Materials* **2015**, *8*, 2276−2296.
(21) Shao, C.; Li, X.; Pei, Z.; Liu, D.; Wang, L.; Dong, H.; Pei, Y. Facile Fabrication of Glycopolymer-based Iron Oxide Nanoparticles and their Applications in the Carbohydrate-Lectin Interaction and Targeted Cell Imaging. *Polym. Chem.* **2016**, *7*, 1337−1344.
(22) Fratila, R. M.; Moros, M.; de la Fuente, J. M. Recent Advances in Biosensing Using Magnetic Glyconanoparticles. *Anal. Bioanal. Chem.* **2016**, *408*, 1783−1803.
(23) Le-Masurier, S. P.; Duong, H. T. T.; Boyer, C.; Granville, A. M. Surface Modification of Polydopamine Coated Particles *via* Glycopolymer Brush Synthesis for Protein Binding and FLIM Testing. *Polym. Chem.* **2015**, *6*, 2504−2511.
(24) Santoyo-Gonzalez, F.; Hernandez-Mateo, F. Silica-based Clicked Hybrid Glyco Materials. *Chem. Soc. Rev.* **2009**, *38*, 3449−3462.
(25) Ahire, J. H.; Behray, M.; Webster, C. A.; Wang, Q.; Sherwood, V.; Saengkrit, N.; Ruktanonchai, U.; Woramongkolchai, N.; Chao, Y. Synthesis of Carbohydrate Capped Silicon Nanoparticles and Their Reduced Cytotoxicity, *in vivo* Toxicity and Cellular Uptake. *Adv. Healthcare Mater.* **2015**, *4*, 1877−1886.
(26) Stenzel, M. H.; Zhang, L.; Huck, W. T. S. Temperature-Responsive Glycopolymer Brushes Synthesized via RAFT Polymerization Using the Z-group Approach. *Macromol. Rapid Commun.* **2006**, *27*, 1121−1126.
(27) Pan, Y.; Ma, C.; Tong, W.; Fan, C.; Zhang, Q.; Zhang, W.; Tian, F.; Peng, B.; Qin, W.; Qian, X. Preparation of Sequence-Controlled Triblock Copolymer-Grafted Silica Microparticles by Sequential-ATRP for Highly Efficient Glycopeptides Enrichment. *Anal. Chem.* **2015**, *87*, 656−662.
(28) An, J.; Zhang, X.; Guo, Q.; Zhao, Y.; Wu, Z.; Li, C. Glycopolymer Modified Magnetic Mesoporous Silica Nanoparticles for MR Imaging and Targeted Drug Delivery. *Colloids Surf., A* **2015**, *482*, 98−108.
(29) Li, D.; Sheng, X.; Zhao, B. Environmentally responsive "hairy" nanoparticles: Mixed homopolymer brushes on silica nanoparticles synthesized by living radical polymerization techniques. *J. Am. Chem. Soc.* **2005**, *127*, 6248−6256.
(30) Bartholome, C.; Beyou, E.; Bourgeat-Lami, E.; Chaumont, P.; Lefebvre, F.; Zydowicz, N. Nitroxide-Mediated Polymerization of Styrene Initiated from the Surface of Silica Nanoparticles. *in situ* Generation and Grafting of Alkoxyamine Initiators. *Macromolecules* **2005**, *38*, 1099−1106.
(31) Yokoyama, R.; Suzuki, S.; Shirai, K.; Yamauchi, T.; Tsubokawa, N.; Tsuchimochi, M. Preparation and Properties of Biocompatible Polymer-Grafted Silica Nanoparticle. *Eur. Polym. J.* **2006**, *42*, 3221−3229.
(32) Radhakrishnan, B.; Ranjan, R.; Brittain, W. J. Surface Initiated Polymerizations from Silica Nanoparticles. *Soft Matter* **2006**, *2*, 386−396.
(33) Glogowski, E.; Tangirala, R.; Russell, T. P.; Emrick, T. Functionalization of Nanoparticles for Dispersion in Polymers and Assembly in Fluids. *J. Polym. Sci., Part A: Polym. Chem.* **2006**, *44*, 5076−5086.
(34) Liu, J.; Tanaka, T.; Sivula, K.; Alivisatos, A. P.; Fréchet, J. M. Employing End-Functional Polythiophene to Control the Morphology of Nanocrystal Polymer Composites in Hybrid Solar Cells. *J. Am. Chem. Soc.* **2004**, *126*, 6550−6551.
(35) Yeole, N.; Kutcherlapati, S. R.; Jana, T. Tunable Core-Shell Nanoparticles: Macro-RAFT Mediated One Pot Emulsion Polymerization. *RSC Adv.* **2014**, *4*, 2382−2388.
(36) Yeole, N.; Kutcherlapati, S. R.; Jana, T. Polystyrene-Graphene Oxide (GO) Nanocomposite Synthesized by Interfacial Interactions Between RAFT Modified GO and Core-Shell Polymeric Nanoparticles. *J. Colloid Interface Sci.* **2015**, *443*, 137−142.
(37) Hill, M. R.; Carmean, R. N.; Sumerlin, B. S. Expanding the Scope of RAFT Polymerization: Recent Advances and New Horizons. *Macromolecules* **2015**, *48*, 5459−5469.
(38) Moad, G.; Rizzardo, E.; Thang, S. H. Living Radical Polymerization by the RAFT Process-a third update. *Aust. J. Chem.* **2012**, *65*, 985−1076.
(39) Darcos, V.; Duréault, A.; Taton, D.; Gnanou, Y.; Marchand, P.; Caminade, A. M.; Majoral, J. P.; Destarac, M.; Leising, F. Synthesis of Hybrid Dendrimer-Star Polymers by the RAFT Process. *Chem. Commun.* **2004**, *18*, 2110−2111.
(40) Moad, G.; Rizzardo, E.; Thang, S. H. Living Radical Polymerization by the RAFT Process. *Aust. J. Chem.* **2005**, *58*, 379−410.
(41) Mc Cormick, C. L.; Lowe, A. B. Aqueous RAFT Polymerization: Recent Developments in Synthesis of Functional Water Soluble Polymers with Controlled Structures. *Acc. Chem. Res.* **2004**, *37*, 312−325.
(42) Li, C.; Han, J.; Ryu, C. Y.; Benicewicz, B. C. A Versatile Method to Prepare RAFT Agent Anchored Substrates and the Preparation of PMMA Grafted Nanoparticles. *Macromolecules* **2006**, *39*, 3175−3183.
(43) Pyun, J.; Jia, S.; Kowalewski, T.; Patterson, G. D.; Matyjaszewski, K. Synthesis and Characterization of Organic/Inorganic Hybrid Nanoparticles: Kinetics of Surface-Initiated Atom Transfer Radical Polymerization and Morphology of Hybrid Nanoparticle Ultrathin Films. *Macromolecules* **2003**, *36*, 5094−5104.
(44) Agrawal, B. B.; Goldstein, I. J. Specific Binding of Concanavalin A to Cross-linked Dextran Gels. *Biochem. J.* **1965**, *96*, 23C−35C.
(45) Bhanu, K.; Komath, S. S.; Maiya, B. G.; Swamy, M. J. Interaction of Porphyrins with Concanavalin A and Pea Lectin. *Curr. Sci.* **1997**, *73*, 598−602.
(46) Sultan, N. A. M.; Swamy, M. J. Energetics of Carbohydrate Binding to Momordica charantia (bitter gourd) Lectin: An Isothermal Titration Calorimetric Study. *Arch. Biochem. Biophys.* **2005**, *437*, 115−125.
(47) Pati, D.; Shaikh, A. Y.; Das, S.; Nareddy, P. K.; Swamy, M. J.; Hotha, S.; Gupta, S. S. Controlled Synthesis of O-Glycopolypeptide Polymers and Their Molecular Recognition by Lectins. *Biomacromolecules* **2012**, *13*, 1287−1295.
(48) Stöber, W.; Fink, A.; Bohn, E. Controlled Growth of Monodisperse Silica Spheres in the Micron Size Range. *J. Colloid Interface Sci.* **1968**, *26*, 62−69.
(49) Mitsukami, Y.; Donovan, M. S.; Lowe, A. B.; McCormick, C. L. Water-soluble Polymers. 81. Direct Synthesis of Hydrophilic Styrenic-based Homopolymers and Block Copolymers in Aqueous Solution via RAFT. *Macromolecules* **2001**, *34*, 2248−2256.
(50) Chong, Y.; Krstina, J.; Le, T. P.; Moad, G.; Postma, A.; Rizzardo, E.; Thang, S. H. Thiocarbonylthio Compounds [SC (Ph) S− R] in Free Radical Polymerization with Reversible Addition-Fragmentation Chain Transfer (RAFT Polymerization). Role of the Free-Radical Leaving Group (R). *Macromolecules* **2003**, *36*, 2256−2272.
(51) Warren, N. J.; Mykhaylyk, O. O.; Mahmood, D.; Ryan, A. J.; Armes, S. P. RAFT Aqueous Dispersion Polymerization Yields Poly (ethylene glycol)-based Diblock Copolymer Nano-Objects with

DOI: 10.1021/acs.macromol.7b01265
Macromolecules XXXX, XXX, XXX−XXX

Predictable Single Phase Morphologies. *J. Am. Chem. Soc.* **2014**, *136*, 1023−1033.
(52) Bartholome, C.; Beyou, E.; Bourgeat-Lami, E.; Chaumont, P.; Zydowicz, N. Nitroxide-Mediated Polymerization of Styrene Initiated from the Surface of Fumed Silica: Comparison of Two Synthetic Routes. *Polymer* **2005**, *46*, 8502−8510.
(53) Duréault, A.; Taton, D.; Destarac, M.; Leising, F.; Gnanou, Y. Synthesis of Multifunctional Dithioesters using Tetraphosphorus Decasulfide and their Behavior as RAFT agents. *Macromolecules* **2004**, *37*, 5513−5519.
(54) Zheng, Q.; Pan, C. Y. Synthesis and Characterization of Dendrimer-Star Polymer using Dithiobenzoate-Terminated Poly (propylene imine) Dendrimer via Reversible Addition-Fragmentation Transfer Polymerization. *Macromolecules* **2005**, *38*, 6841−6848.
(55) Taniguchi, T.; Kunisada, Y.; Shinohara, M.; Kasuya, M.; Ogawa, T.; Kohri, M.; Nakahira, T. Preparation of Glycopolymer Hollow Particles by Sacrificial Dissolution of Colloidal Templates. *Colloids Surf., A* **2010**, *369*, 240−245.
(56) Schwarz, F. P.; Puri, K. D.; Bhat, R. G.; Surolia, A. Thermodynamics of Monosaccharide Binding to Concanavalin A, Pea (Pisum sativum) Lectin, and Lentil (Lens culinaris) Lectin. *J. Biol. Chem.* **1993**, *268*, 7668−7677.

DOI: 10.1021/acs.macromol.7b01265
Macromolecules XXXX, XXX, XXX−XXX